



Cite this: *Mater. Adv.*, 2023,
4, 1196

Shape deformable hydrogels prepared by altering surface areas with scratching and photolithography patterning methods

Yuanyuan Chen, Yunqi Shi, Min Liang and Huiliang Wang  *

Shape deformable hydrogels have wide potential applications in soft robotics, artificial muscles, manipulators and flexible devices. The development of simple, facile and efficient methods for preparing shape deformable hydrogels is of significant importance for their practical applications. In this work, we proposed a novel strategy to transform isotropic hydrogels into shape deformable hydrogels by altering the surface areas and hence the swelling behaviours of hydrogels. Simple scratching and photolithography patterning methods are employed to introduce grooves or projections on the surface of hydrogels. By controlling the density and direction of scratches, or the width, density, height and direction of the stripes, the degree and direction of the bending and twisting of the hydrogel can be adjusted. Taking the advantages of the photolithography method, more precise and complex patterns can be introduced onto hydrogel samples with different shapes; therefore, more complex shape deformations from 2D to 3D can be achieved. The strategy of changing surface area to endow isotropic hydrogels with shape deformation behaviour can be applied to a wide variety of hydrogels and many methods can be employed; therefore, it is of great significance for many practical applications.

Received 22nd November 2022,
Accepted 13th January 2023

DOI: 10.1039/d2ma01052f

rsc.li/materials-advances

Introduction

Living beings in nature can undergo intelligent and controllable movements or shape deformations upon exposure to external stimuli. Typical examples include plants like Venus flytraps that close their leaves to capture prey by the redistribution of water¹ and Bauhinia variegata that disperses seeds by rapidly opening its flat pod upon dehydration,² and animals like an inchworm that walks through the bending/unbending of its body³ and a jellyfish that swims by shrinking its umbrella-shaped body and squeezing out water.⁴ Inspired by plants and animals, intelligent actuators that can undergo geometric shape deformations upon exposure to external stimuli have been developed.⁵ Shape deformable hydrogels have attracted great research interest in recent years, as they have wide potential applications in flexible devices, soft robotics, manipulators and artificial muscles.⁶

Shape deformation or movement of hydrogels is generally driven by the nonuniform volume expansion/contraction induced by external stimuli or the anisotropic structure of the hydrogels. Hydrogels with isotropic structures commonly undergo uniform volume expansion/contraction upon swelling/deswelling under external stimuli. They can only undergo shape deformations

when a nonuniform external stimulus like local light irradiation⁷ is applied or its structure (e.g., electrically charged ions) and hence water distribution in the hydrogel can be changed under an applied electric field.⁸ On the other hand, hydrogels with inherent anisotropic structures can undergo shape deformations upon exposure to uniform stimuli due to the uneven swelling/deswelling of the different parts of the hydrogels, and very complex deformations can be easily achieved by adjusting the structures of hydrogels. Therefore, the preparation of anisotropic shape-deformable hydrogels has attracted more and more attention.

Anisotropic shape-deformable hydrogels can be mainly divided into four categories: bilayer hydrogels,⁹ gradient hydrogels,¹⁰ patterned hydrogels,¹¹ and hydrogels with oriented structures.¹² Bilayer and gradient hydrogels generally undergo simple bending/unbending deformations, and hydrogels with oriented structures undergo expansion/contraction in one direction. Patterned hydrogels are able to perform more complex deformations, since patterned regions with different response rates and degrees can be introduced into the hydrogels by changing the local compositions and/or crosslinking densities of the hydrogels. Photolithographic,¹³ electrochemical ion-printing,¹⁴ ion-transfer-printing,¹⁵ ion-inkjet-printing,¹⁶ electrochemical reduction¹⁷ and other methods are developed or employed to introduce structural inhomogeneity into as-prepared isotropic hydrogels.

The anisotropic shape deformable hydrogels can also be categorized into different types based on their structural heterogeneities

Beijing Key Laboratory of Energy Conversion and Storage Materials, College of Chemistry, Beijing Normal University, Beijing 100875, P. R. China.
E-mail: wanghl@bnu.edu.cn



in one or more dimensions of hydrogel samples. For the bilayer and gradient hydrogels, structural heterogeneity exists in the composition and/or crosslinking density along the thickness direction, for the photolithographically patterned hydrogels and hydrogels with oriented structures, in-plane structural heterogeneity exists. And for the patterned hydrogels prepared with various ion-printing and electrochemical reduction methods, both in-plane and in-thickness structural heterogeneities exist. In fact, in-plane and in-thickness structural heterogeneities exist only in a very thin surface layer of some hydrogels, but they are sufficient to induce shape deformations, as the swelling/deswelling properties of the hydrogels are largely determined by their surface layers.

Up to now, the methods for preparing shape deformable hydrogels especially those with complex shape deformations are generally complicated and require specific equipment. The development of simple, facile and efficient methods to prepare hydrogels with complex and controllable deformations is of great significance for the wider applications of deformable hydrogels. In this work, we propose a novel strategy of preparing shape deformable hydrogels by altering their surface areas with an extremely simple scratching method and a photolithography patterning method. The change in surface area leads to a change in swelling behaviour of the hydrogels. Complex shape deformations of hydrogels can be achieved by introducing patterned grooves or projections on the surfaces of the hydrogels.

Results and discussion

Shape deformation of scratched hydrogels

By introducing scratches on the surface of the hydrogels, they can undergo shape deformation when immersed in water. As shown in Fig. 1, hydrogel stripes with scratches in different directions undergo twisting and bending deformations in deionized water. When the scratches are in directions 30° and 45° to the direction of the hydrogel length side, the gel stripes twist into a helix shape with 2 and 4 spiral circles, respectively (Fig. 1a and b); while when the scratches are in 90° and 180° directions, the gel stripes deform into circles (Fig. 1c and d).

To understand the origin of the bending deformation of scratched hydrogels in deionized water, we observed the surface morphology of the as-prepared and scratched hydrogels

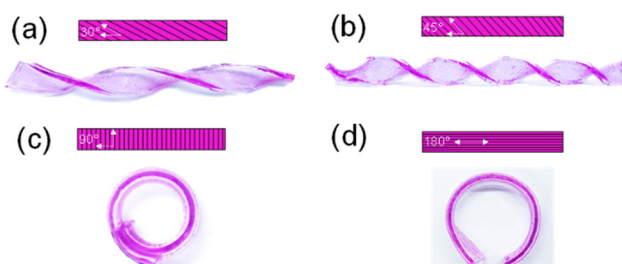


Fig. 1 Deformation of the hydrogel stripes ($5 \text{ mm} \times 1 \text{ cm} \times 1 \text{ mm}$) with scratches in the directions 30° (a), 45° (b), 90° (c) and 180° (d) to the direction of the hydrogel length side after swelling in deionized water for 2 min.

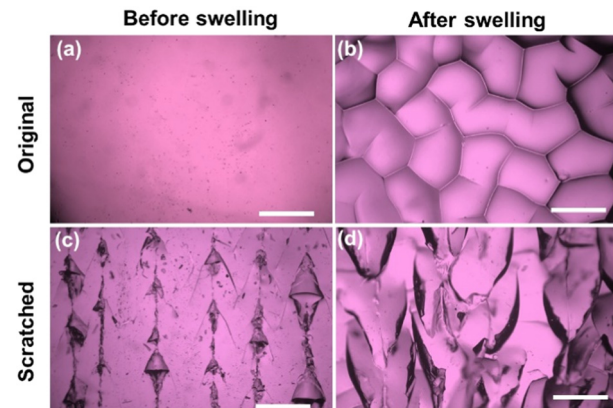


Fig. 2 Surface morphology of the original (a and b) and scratched (c and d) hydrogels before (a and c) and after (b and d) swelling in water for 2 min. Scale: 1 mm.

before and after swelling. As shown in Fig. 2, the as-prepared hydrogel has a smooth surface, while the scratched hydrogel shows aligned but irregular scratches on the surface. After swelling in water for a short time (2 min), randomly distributed wrinkles appear on the surface of the original hydrogel due to internal stress induced by the faster swelling of the hydrogel in the surface layer than the inner part. When the scratched hydrogel is swelled in water, it shows a surface morphology with aligned scratches larger than those on the hydrogel before swelling. That is, anisotropic swelling occurs along the direction of the scratches ($\times 1 \text{ mm}$) with different numbers of scratches when immersed in water for different times. As shown in Fig. 3, the swelling ratio of the original hydrogel without scratches is always smaller than those of the scratched hydrogels, and for the hydrogels with scratches the swelling ratio increases with the increase of the scratch number and the difference becomes larger with the increase of time.

Therefore, for the hydrogel stripes with scratches on one side, the difference in the swelling rate and swelling degree between the scratched side and the unscratched side will lead to the bending of the hydrogel strip towards the less swollen side (unscratched side). For the hydrogel stripes with scratches

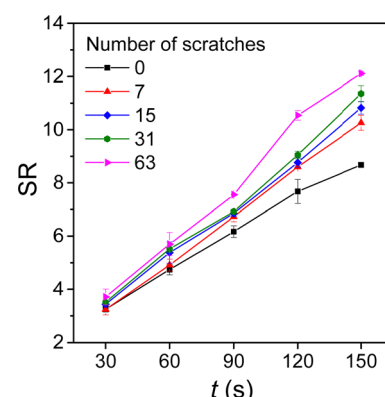


Fig. 3 The change of swelling ratios of the hydrogel stripes ($1.5 \text{ cm} \times 6 \text{ mm} \times 1 \text{ mm}$) with different numbers of scratches with swelling time.



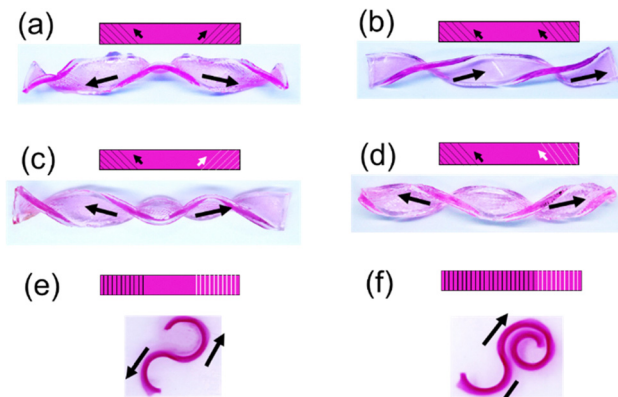


Fig. 4 Deformation of hydrogel stripes in deionized water for 2 min after introducing different scratches in different directions on the same side (a and b) and different sides (c–f) of the hydrogel stripes.

in different directions, the anisotropic swelling along the direction of the scratches leads to the twisting or bending of the hydrogel stripes (Fig. 1).

More complex shape deformations of hydrogels can be obtained by introducing scratches in different directions and of varying densities onto different locations and/or sides of hydrogel stripes. As shown in Fig. 4, when the two ends of a hydrogel strip are engraved with symmetrical oblique scratches (45° and 135° , Fig. 4a and c) or scratches in the same direction (45° , Fig. 4b and d) on the same side (Fig. 4a and b) or different sides (Fig. 4c and d), respectively, the hydrogel strips twist into different symmetrical or asymmetrical spiral shapes with the two ends twisted towards opposite or the same directions. When the two ends of a hydrogel strip are engraved with symmetrical longitudinal scratches (90°) on different sides, the two ends of the hydrogel strip bend towards opposite directions and hence an “S” shape is formed (Fig. 4e). When different numbers of longitudinal scratches are cut on the two ends of different sides, the end with more scratches bends more significantly and the hydrogel deforms into a shape similar to a musical note – the treble clef (Fig. 4f).

Swelling behaviour of photolithography patterned hydrogels

The scratching method is capable of altering the surface area of hydrogels and hence their swelling behaviours, which leads to the shape deformation of hydrogels. Although this method is extremely simple and effective, unfortunately, it is difficult to produce uniform scratches by cutting, and hence, it cannot precisely control the surface area of the hydrogels. To overcome the drawback of the scratching method, we developed a photolithography patterning (PLP) method to form patterned structures with accurate length, width, density and thickness on the hydrogel surface. Therefore, this PLP method is able to control the surface areas of the hydrogels and hence their swelling behaviours and shape deformations.

We prepared hydrogel samples ($6\text{ cm} \times 2\text{ cm} \times 1\text{ mm}$) with photolithographed rectangular stripes. The definition of the width (a), length (b), height (h) and the distance (d) between the

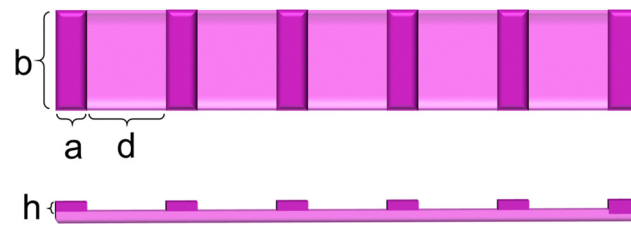


Fig. 5 The definition of the width (a), length (b), height (h) of stripes on the surface of a hydrogel sample and the distance (d) between the stripes.

stripes is shown in Fig. 5. The length (a) of the stripes is always 2 cm, while one of the structural parameters, *i.e.*, width (a) or height (h) of the stripes or the distance (d) between them, is varied, with the other two remaining constant at 2 mm, 1 mm or 4 mm, respectively.

The swelling behaviours of the hydrogels with photolithographed stripes were measured and the change of the swelling ratio (SR) with the swelling time is shown in Fig. 6. At the same swelling time, the SR of the hydrogel samples increases with the increase of the height of the stripes, and the difference in the SR becomes larger with the increase of swelling time (Fig. 6a). The increase of the stripe height leads to the increase of the lateral area of the stripes and hence the total surface area of the gel sample, which leads to the faster swelling and a higher SR of the gel sample. The SR of the hydrogel samples decreases with the increase of the width of the stripes (Fig. 6b), while it does not change significantly with the change of the distance between the stripes in the measured ranges (Fig. 6c). The increase of width of the stripes does not increase the surface area of the hydrogel sample, while the decrease of the distance between the stripes leads to an increase of the number

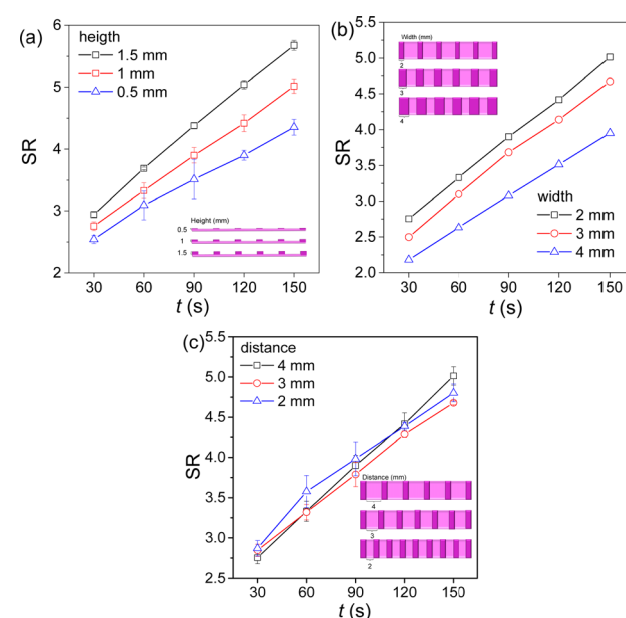


Fig. 6 The change of the swelling ratios of the hydrogels with photolithographed stripes of different heights (a), widths (b) and distances (c) with swelling time in water.



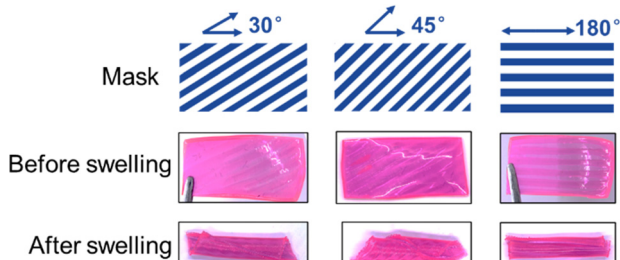


Fig. 7 Designed masks, photolithographed hydrogel samples with stripes in different angles and their deformations after swelling in deionized water for 2 min.

of stripes and hence the surface area of the hydrogels. However, the SR of the hydrogels decreases or does not change significantly. The very possible reason is that the introduction of stripes on the hydrogels increases the crosslinking density of the photolithographed regions, leading to the decreased swelling ratios of the hydrogels.

Shape deformation of photolithography patterned hydrogels

Hydrogel samples with photolithographed stripes can also undergo shape deformations when immersed in water. The size of the rectangular gel samples is $4\text{ cm} \times 2\text{ cm} \times 1\text{ mm}$, and the width and thickness of the stripes are 2 mm. The angles of the stripes are 30° , 45° and 180° to the length direction of the hydrogel samples. As shown in Fig. 7, when the angle is 30° or 45° , the gel samples twist into a helix shape, and when the angle is 180° , the gel curls into a tube along the length direction.

To increase the surface area and especially the lateral area of the patterns, we introduced row(s) of hydrogel cylinders to replace stripes on the hydrogel samples. When one row of circular hydrogel cylinders is photolithographed in the middle of a square hydrogel sample, the hydrogel undergoes bending after swelling in water (Fig. 8a); when two rows of parallel hydrogel cylinders are photolithographed, the hydrogel deforms into a triangular prism upon swelling (Fig. 8b); and when two rows of hydrogel cylinders are photolithographed on the diagonal lines of the hydrogel, the hydrogel deforms into a flower with four petals (Fig. 8c).

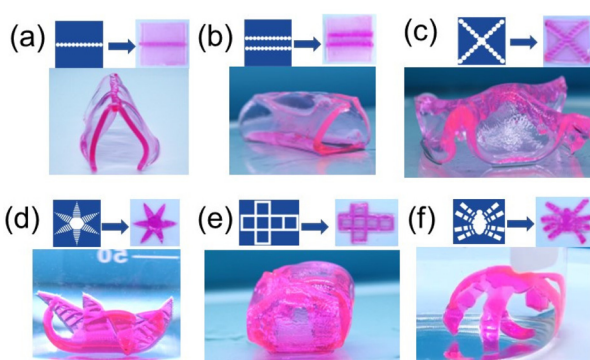


Fig. 8 Designed masks, photolithographed hydrogel samples and their deformations after swelling in deionized water for 2 min (a–c and e) or 5 s (d and f).

More complex shape deformations can also be achieved by using hydrogel samples with different shapes and photolithographed patterns on them. For example, when stripes are photographed on the petals of a flower-like two-dimensional hydrogel sample, the petals of the flower will hold together like Mimosa (Fig. 8d), a hydrogel sample photographed with a cube's affirmative pattern folds into a three-dimensional cube shape (Fig. 8e), and a flat spider-shaped hydrogel sample with photolithographed hydrogel stripes on the legs will deform into a standing spider (Fig. 8f).

Conclusions

In this work, we developed scratching and photolithography patterning (PLP) methods to prepare hydrogels with controllable and complex shape deformations. Introducing grooves or projections to one surface or different parts of two surfaces of the hydrogel samples by these methods leads to the increased surface area(s) of the treated parts, and the difference in the surface areas of two sides or different parts of one or two sides results in their different swelling rates and swelling ratios, and hence the shape deformations of the hydrogel samples. By controlling the density and direction of the scratches, or the width, density, height and direction of the stripes, the degree and direction of the bending and twisting of the hydrogel can be adjusted. Taking the advantages of the photolithography method, more precise and complex patterns can be introduced onto hydrogel samples with different shapes, therefore more complex shape deformations from 2D to 3D can be achieved. Compared with some other methods for preparing shape deformable hydrogels, the scratching method is extremely simple and effective in transforming an isotropic hydrogel into an anisotropic shape deformable hydrogel. And the PLP method is also effective in introducing structural inhomogeneity onto the surface of the hydrogel. The idea of changing surface area to endow hydrogels with shape deformation behaviour can be applied to a wide variety of hydrogels and many methods can be employed; therefore, it should be of great significance for many practical applications.

Experimental

Materials and equipment

Acrylamide (AAm, 99%) and polyvinyl pyrrolidone (PVP, $M_w = 4.0 \times 10^4$) were purchased from Amresco Inc. (OH, USA), acrylic acid (AA, 99%) and 2-hydroxy-4'-(2-hydroxyethoxy)-2-methylpropiophenone (2959, 98%) were purchased from Aladdin Reagent Co. Ltd (Shanghai, China), *N,N'*-methylenebisacrylamide (MBAA, 99%) and potassium persulfate (KPS, 99%) were purchased from Beijing InnoChem Science & Technology Co. Ltd (Beijing, China), sodium hydroxide (NaOH, AR) was purchased from Beijing Chemical Reagent Factory (Beijing, China), and Rhodamine B was purchased from Alfa Aesar (Tianjin, China). All chemicals were used as received without further purification. Deionized water was used for all experiments. The UV system with a shutter assembly and an air-cooling fan was supplied by RunWing



(Shenzhen, China). The UVC intensity at the reaction site was 12 mW cm⁻².

Hydrogel preparation

The hydrogel system used in this work is similar to that reported in our previous work.¹⁵ A solution containing PVP (43 mg mL⁻¹), the monomers AAM (3 mol L⁻¹) and NaAAc (0.3 mol L⁻¹), the photo-initiator 2959 and the cross-linking agent MBAA (both 0.1 mol% to the monomers) as well as Rhodamine B (3.0×10^{-4} mol L⁻¹) was prepared. At a low temperature (ice bath), the solution was bubbled with high-purity nitrogen (about 15 min) to remove dissolved oxygen. Then, the solution was injected into a mold by placing a silicone spacer with a height of 1 mm between two quartz plates. Finally, the mold was sealed and placed under the irradiation of UV light for 3 min to obtain a hydrogel.

Preparation of deformable hydrogel by scratching and photolithography patterning

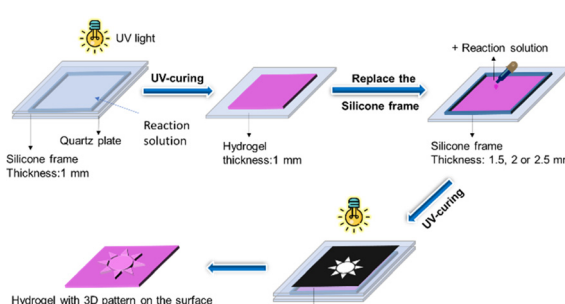
Scratching method. Different scratches were directly scratched on the gel surface with a sharp knife.

Photolithography-patterning (PLP) method. As shown in Scheme 1, after the preparation of the hydrogel sample in Section 2.2, one quartz plate and the silicone frame were removed, leaving the gel on the other quartz plate intact. Then another silicone frame with a thickness of 1.5, 2 or 2.5 mm was used. The solution used for preparing hydrogels in Section 2.2 was poured directly onto the gel surface and then sealed with a quartz glass plate. A transparent film with printed patterns was pasted on the surface of the quartz glass, and then photopolymerization was carried out. Finally, the patterned hydrogel was removed from the mould gently and the unreacted solution was removed.

Swelling behaviour of hydrogels

The swelling behaviour of the original hydrogel and the scratched hydrogels were measured by weighing the hydrogel samples (original size: 1.5 cm × 6 mm × 1 mm) immersed in deionized water at room temperature for different periods. The swelling ratio (SR) of the hydrogel was calculated by the following equation:

$$SR = \frac{m_s - m_d}{m_d}$$



Scheme 1 Schematic process of preparing shape deformable hydrogels by photolithography-patterning method.

where m_s is the weight of the swollen hydrogel, and m_d is the weight of the vacuum-dried hydrogel sample.

Adjusting shape deformation of hydrogels by scratching and PLP methods

For the scratching method, the shape deformation of hydrogels was adjusted by cutting scratches in different directions, densities and styles as well as on different sides of the hydrogels.

For the PLP method, computer-designed patterns like simple stripes with different widths, distances, and angles as well as complex patterns were printed on transparent films, and then the films were used as masks for photopolymerization to introduce patterns on hydrogels. These hydrogels underwent different shape deformations. By controlling the thickness of the silicone frame, the thickness of the introduced pattern could be adjusted to further control the degree of deformation of the hydrogel.

Conflicts of interest

There are no conflicts to declare.

Acknowledgements

We thank the financial support from the National Natural Science Foundation of China (Grant No. 21875023) and the Program for Changjiang Scholars and Innovative Research Team (PCSIRT) in University.

Notes and references

- Y. Forterre, J. M. Skotheim, J. Dumais and L. Mahadevan, *Nature*, 2005, **433**, 421–425.
- S. Armon, E. Efrati, R. Kupferman and E. Sharon, *Science*, 2011, **333**, 1726–1730.
- W. Wang, J.-Y. Lee, H. Rodrigue, S.-H. Song, W.-S. Chu and S.-H. Ahn, *Bioinspiration Biomimetics*, 2014, **9**, 046006.
- J. C. Nawroth, H. Lee, A. W. Feinberg, C. M. Ripplinger, M. L. McCain, A. Grosberg, J. O. Dabiri and K. K. Parker, *Nat. Biotechnol.*, 2012, **30**, 792–797.
- L. Ionov, *Adv. Funct. Mater.*, 2013, **23**, 4555–4570; L. Ionov, *Langmuir*, 2015, **31**, 5015–5024; S.-J. Jeon, A. W. Hauser and R. C. Hayward, *Acc. Chem. Res.*, 2017, **50**, 161–169; R. Kempaiah and Z. H. Nie, *J. Mater. Chem. B*, 2014, **2**, 2357–2368.
- X. Peng and H. L. Wang, *J. Polym. Sci., Part B: Polym. Phys.*, 2018, **56**, 1314–1324; R. Li, D. D. Jin, D. Pan, S. Y. Ji, C. Xin, G. L. Liu, S. Y. Fan, H. Wu, J. W. Li, Y. L. Hu, D. Wu, L. Zhang and J. R. Chu, *ACS Nano*, 2020, **14**, 5233–5242; Z. C. Sun, C. Y. Song, J. J. Zhou, C. B. Hao, W. T. Liu, H. Liu, J. F. Wang, M. M. Huang, S. Q. He and M. C. Yang, *Macromol. Rapid Commun.*, 2021, **42**, 2100499; Z. X. Xu and J. Fu, *ACS Appl. Mater. Interfaces*, 2020, **12**, 26476–26484; Y. S. Zhao, C. Xuan, X. S. Qian, Y. Alsaad, M. T. Hua, L. H. Jin and X. M. He, *Sci. Rob.*, 2019, **4**, eaax7112; Q. L. Zhu, C. Du, Y. H. Dai, M. Daab, M. Matejdes, J. Breu, W. Hong, Q. Zheng and Z. L. Wu, *Nat. Commun.*, 2020, **11**, 5166.



7 X. Peng, T. Liu, C. Jiao, Y. Wu, N. Chen and H. Wang, *J. Mater. Chem. B*, 2017, **5**, 7997–8003; T. Chen, H. Li, Z. Li, Q. Jin and J. Ji, *Mater. Horiz.*, 2016, **3**, 581–587; L. Huang, R. Jiang, J. Wu, J. Song, H. Bai, B. Li, Q. Zhao and T. Xie, *Adv. Mater.*, 2017, **29**, 1605390; P. Palffy-Muhoray, *Nat. Mater.*, 2009, **8**, 614–615.

8 Y. Osada and A. Matsuda, *Nature*, 1995, **376**, 219.

9 Z. Hu, X. Zhang and Y. Li, *Science*, 1995, **269**, 525–527; C. Yao, Z. Liu, C. Yang, W. Wang, X.-J. Ju, R. Xie and L.-Y. Chu, *Adv. Funct. Mater.*, 2015, **25**, 2980–2991; C. Ma, W. Lu, X. Yang, J. He, X. Le, L. Wang, J. Zhang, M. J. Serpe, Y. Huang and T. Chen, *Adv. Funct. Mater.*, 2018, **28**, 1704568; S. Liu, G. Gao, Y. Xiao and J. Fu, *J. Mater. Chem. B*, 2016, **4**, 3239–3246; L. Zhao, J. Huang, Y. Zhang, T. Wang, W. Sun and Z. Tong, *ACS Appl. Mater. Interfaces*, 2017, **9**, 11866–11873; P. Sun, H. Zhang, D. Xu, Z. W. Wang, L. F. Wang, G. R. Gao, G. Hossain, J. Y. Wu, R. Wang and J. Fu, *J. Mater. Chem. B*, 2019, **7**, 2619–2625; Q. L. Wang, Z. Liu, C. Tang, H. Sun, L. Zhu, Z. Z. Liu, K. Li, J. Yang, G. Qin, G. Z. Sun and Q. Chen, *ACS Appl. Mater. Interfaces*, 2021, **13**, 10457–10466; S. Z. Zhou, B. Y. Wu, Q. Zhou, Y. K. Jian, X. X. Le, H. H. Lu, D. C. Zhang, J. W. Zhang, Z. H. Zhang and T. Chen, *Macromol. Rapid Commun.*, 2020, **41**, 1900543.

10 C. Y. Li, X. P. Hao, Z. L. Wu and Q. Zheng, *Chem. – Asian J.*, 2019, **14**, 94–104; K. W. Mo, J. H. Lin, P. Wei, J. Mei and C. Y. Chang, *J. Mater. Chem. C*, 2021, **9**, 10295–10302; Z. J. Wang, W. Hong, Z. L. Wu and Q. Zheng, *Angew. Chem., Int. Ed.*, 2017, **56**, 15974–15978.

11 M. Shojaeifard, S. Niroumandi and M. Baghani, *Acta Mech.*, 2022, **233**, 213–232; Y. Sui, C. C. Li, S. Y. Feng, Y. Ling, C. Li, X. S. Wu, J. H. Shen, J. Song, H. L. Peng and W. G. Huang, *J. Mater. Chem. A*, 2021, **9**, 8586–8597; J. D. Tang, L. S. Zeng and Z. S. Liu, *Soft Matter*, 2021, **17**, 8059–8067; Q. L. Zhu, C. F. Dai, D. Wagner, O. Khoruzhenko, W. Hong, J. Breu, Q. Zheng and Z. L. Wu, *Adv. Sci.*, 2021, **8**, 2102353.

12 M. J. Liu, Y. Ishida, Y. Ebina, T. Sasaki, T. Hikima, M. Takata and T. Aida, *Nature*, 2015, **517**, 68–72.

13 H. Therien-Aubin, Z. L. Wu, Z. Nie and E. Kumacheva, *J. Am. Chem. Soc.*, 2013, **135**, 4834–4839; Z. L. Wu, M. Moshe, J. Greener, H. Therien-Aubin, Z. Nie, E. Sharon and E. Kumacheva, *Nat. Commun.*, 2013, **4**, 1586; Z. J. Wang, C. N. Zhu, W. Hong, Z. L. Wu and Q. Zheng, *J. Mater. Chem. B*, 2016, **4**, 7075–7079; Z. J. Wang, W. Hong, Z. L. Wu and Q. Zheng, *Angew. Chem., Int. Ed.*, 2017, **56**, 15974–15978.

14 E. Palleau, D. Morales, M. D. Dickey and O. D. Velev, *Nat. Commun.*, 2013, **4**, 2257; B. P. Lee and S. Konst, *Adv. Mater.*, 2014, **26**, 3415–3419; B. P. Lee, M.-H. Lin, A. Narkar, S. Konst and R. Wilharm, *Sens. Actuators, B*, 2015, **206**, 456–462; B. P. Lee, A. Narkar and R. Wilharm, *Sens. Actuators, B*, 2016, **227**, 248–254.

15 X. Peng, Y. Li, Q. Zhang, C. Shang, Q.-W. Bai and H. Wang, *Adv. Funct. Mater.*, 2016, **26**, 4491–4500.

16 X. Peng, T. Liu, Q. Zhang, C. Shang, Q.-W. Bai and H. Wang, *Adv. Funct. Mater.*, 2017, **27**, 1701962.

17 X. Peng, C. Jiao, Y. Zhao, N. Chen, Y. Wu, T. Liu and H. Wang, *ACS Appl. Nano Mater.*, 2018, **1**, 1522–1530.

